Polym. Bull. (2010) 64:471–481
DOI 10.1007/s00289-009-0191-3

ORIGINAL PAPER

Crystallization, hydrolytic degradation, and mechanical properties of poly (trimethylene terephthalate)/poly(lactic acid) blends

Hantao Zou · Changhai Yi · Luoxin Wang · Weilin Xu

Received: 23 May 2009 / Revised: 4 August 2009 / Accepted: 8 October 2009 /

Abstract Crystallization, melting, hydrolytic degradation, and mechanical properties of poly(trimentylene terephthalate)/poly(lactic acid) (PTT/PLA) blends have been investigated. The blends show a single and composition-dependent glass-transition temperature ($T_{g)}$ over the entire composition range, implying that these blends are fully miscible in the amorphous state. The observed T_g is found to increase with increasing PLA content and fitted well with the Gordon–Taylor equation, with the fitting parameter k being 0.91. The cold-crystallization peak temperature increases, while the melt-crystallization peak decreases with increasing the PLA content. Both the pure PTT and PTT/PLA blends cannot accomplish the crystallization during the cooling procedure and the recrystallization occurs again on the second heating. Therefore, on the thermogram recorded, there is exothermal peak followed by endothermal peak with a shoulder. However, to pure PLA, no crystallization takes place during cooling from the melt, therefore, no melting endothermic peak is found on the second heating curve. WAXD analysis indicates PLA and PTT components do not co-crystallize and the crystalline phase of the blends is that of their enriched pure component. With increasing PLA content, the hydrolytic degradation of the blend films increases, while both the tensile strength and the elongation at break of the blend films decrease. That is to say, the hydrolytic degradation of the PTT/PLA blends increases with the introduction of PLA at the cost of the decrease of the flexibility of PTT.

Keywords Poly(lactic acid) (PLA) · Poly(trimethylene terephthalate) (PTT) · Crystallization behavior · Hydrolytic degradation · Mechanical property

---

H. Zou (✉) · C. Yi · L. Wang · W. Xu
Key Laboratory of Green Processing and Functional Textile of New Textile Materials, Ministry of Education, Wuhan University of Science and Engineering, Wuhan, Hubei 430073, People's Republic of China
e-mail: zouhantao@mail.dhu.edu.cn

Introduction

Poly(lactic acid) (PLA) is among the most important biodegradable synthetic polymers owing to its mechanical property, thermoplastic processibility, and biological properties, such as biocompatibility and biodegradability [1]. Therefore, it has received much interest for its medical, pharmaceutical, packing, clothing, and environmental applications [2, 3]. However, PLA belongs to the group of polymers with poor thermal stability and is highly sensitive to heat [4]. Moreover, its processability is not good for industrial processing operations in the case of a homopolymer structure [5]. Blends of PLA with several polymers have been prepared in an effort to enhance the properties of PLA and also to obtain novel materials. PLA has been blended with polyethylene (PE) [6], polypropylene (PP) [7], polystyrene (PS) [8], poly(ethylene glycol) (PEG) [9], poly(caprolactone) (PCL) [10], poly(methyl meth-acrylate) (PMMA) [11], modified carbon black [12], epoxidized soybean oil [13], and so on to obtain materials with improved properties such as toughness, modulus, impact strength, and thermal stability compared to using the pure polymers.

Poly (trimethylene terephthalate) (PTT) is a newly commercialized crystalline polymer with growing applications in fibers, films, and engineering plastic owing to an unusual combination of the outstanding properties of PET and the processing characteristics of PBT. Recently, a considerable amount of research study pertinent to PTT blends was reported in order to broaden the applications of the homopolymer [14–21]. Guerrica et al. [14] found that the toughness of PTT was improved by blending with poly(ethylene–octene) (PEO). Run et al. [15] and Krutphun and Supaphol [16] reported that PTT was miscible with poly(ethylene naphthalate) (PTN) in the amorphous phase, and that the variation in the glass-transition temperature with the blend composition fit the Gordon–Taylor equation well [15, 16]. The correlation of the morphology and rheological response of PTT/m-LLDPE blends was investigated by Jafari et al. [17]. The miscibility, melting, and crystallization behaviors of PTT/PS [18], PTT/PC [19], and PTT/PET [20, 21] blends were reported.

PTT and PLA belong to the polyesters and they have their own advantages and drawbacks. To the best of our knowledge, the blends of PTT and PLA have been rarely studied. In this article, a series of PTT/PLA blends were prepared by melt mixing. The miscibility, crystallization, and melting behaviors of the PTT/PLA blends were studied by DSC and WAXD. The hydrolytic degradation and mechanical property of the blends were also been investigated.

Experimental

Materials and sample preparation

PTT, kindly provided by Yizheng Chemical Fiber Co. Ltd, has an intrinsic viscosity (η) of 0.92 dL/g measured in phenol–tetrachloroethane mixture (1:1, w/w) at 20° using an Ubbelohde viscometer. PLA was obtained from Dikang Zhongke Co. Ltd

(China) with an intrinsic viscosity of 0.685 dL/g in tetrahydrofuran chloroform at 31°.

Prior to melt processing, PTT and PLA were dried in a vacuum oven to less than 60 ppm of moisture content in order to minimize the hydrolytic degradation of the melts. All of the components were thoroughly mixed prior to extrusion. The melt blending of the dried PTT and PLA was carried out using a 30-mm single-screw extruder (Tianhua Institute of Chemical Machinery & Automation, Lanzhou, China) with an L/D (length/diameter) ratio of 36. The barrel temperature ranged from 230 to 250 °C, and the screw speed was 250 rpm. The polymers were mixed to the required weight ratios (PTT/PLA) 100/0, 90/10, 80/20, 70/30, 30/70, 20/80, 10/90, and 0/100.

Characterization

The glass-transition temperature and cold crystallization of PTT, PLA, and PTT/PLA blends were studied using DSC-2910 (Netzsch, Germany) that calibrated with indium prior to performing the measurement, and the weights of all samples were approximately 4 mg. The samples were heated to 250 °C at 100 °C/min under a nitrogen atmosphere, held for 5 min to reset previous thermal histories, after which all of the samples were immediately quenched under a cooling rate of 150 °C/min to obtain the completely amorphous state of six samples, and then heated them to 250 °C with a heating rate of 10 °C/min.

The melt crystallization and subsequent melting behaviors of various binary blends were performed as following: the samples were heated to 250 °C at 100 °C/min under a nitrogen atmosphere, held for 5 min and then cooled to 20 °C at a constant cooling rate of 10 °C/min, and then heated them to 250 °C at a heating rate of 10 °C/min. The cooling process and the second heating process were recorded, respectively.

WAXD measurement was carried out by means of a BRUKER-AXC08 X-ray diffractometer and filtered Cu K radiation ($\lambda = 0.1542$ nm; 40 kV; 40 mA). The diffraction patterns of the blends were obtained by scanning the samples in an interval of $2\theta = 1$–40°.

Hydrolytic degradation was determined with disk-shaped samples with 1 cm diameter, 1 mm thickness, and 100 mg weight by curing presscuring press. Hydrolytic degradations of the products were determined gravimetrically [5]. Thus, the tablets were placed in tubes containing 2 mL of phosphate buffer solution of pH 7.2 and kept in a water bath at 60° for 28 days. The samples were taken out every 7 days, washed with distilled water, and dried under vacuum at 40° for 72 h. The results were given as weight loss%.

The mechanical properties were determined with a Model 5566 Instron Universal Testing Machine (Instron Engineering Corporation, Canton, MA, USA) using an ASTM Method D 638-91. Initial grip separation was set at 50 mm and cross-head speed at 5 mm/min. The results were taken as an average from measurements of at least five specimens.

Results and discussion

Miscibility of PTT/PLA blends

The glass-transition temperature (T_g) was measured on the quenched PTT, PLA, and PTT/PLA blends at a heating rate of 10 °C/min. The T_g s are indicated by the dash in Fig. 1 and listed in Table 1. Obviously, all the blends show a single T_g that depended on the composition. Moreover, the T_g values of the blends locate between those of the pure components ($T_{g,\ PTT} \approx 45$ °C and $T_{g,\ PLA} \approx 62$ °C) and rise monotonically with the increase of PLA content. The presence of a single, composition-dependen T_g of the blends, located between $T_{g,\ PTT}$ and $T_{g,\ PLA}$, indicative of miscibility of PTT and PLA components in the amorphous phase at all blend compositions.

The dependence of T_g on blend composition can be evaluated by the classic Fox equation (1) or Gordon–Taylor equation (2) as follows [21, 22]:

$$\frac{1}{T_g} = \frac{w_1}{T_{g1}} + \frac{w_2}{T_{g2}} \tag{1}$$

$$T_g = \frac{w_1 T_{g1} + k w_2 T_{g2}}{w_1 + k w_2} \tag{2}$$

where subscripts 1 and 2 represent PTT and PLA, respectively; w_i is the weight fractions of component i; and k is an adjustable parameter [21, 22]. Figure 2 shows the measured T_g as a function of PTT content in comparison with the fitting curves of the Fox equation and Gordon–Taylor equation. Apparently, it is noted that measured T_g does not fit well with the predicted T_g value (dotted line as shown in Fig. 2) by the Fox equation. The figure shows that there is over-prediction by the classic Fox model in the entire quaternary blend composition. On the contrary, the solid line predicted according to the Gordon–Taylor equation with the fitting

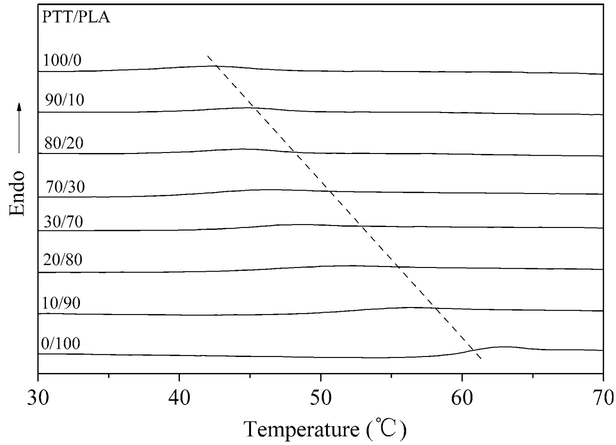

Fig. 1 DSC thermograms for the PTT/PLA blends

Table 1 The glass temperatures, melt-crystallization temperatures, and melting temperatures of PTT/PLA blends

Sample	From quenched scans		From cooling scans		From heating scans	
	T_g (°C)	T_{cc} (°C)	T_{mc} (°C)	$\triangle H_{mc}$ (J/g)	T_m (°C)	$\triangle H_m$ (J/g)
PTT	45.0	85.0	169.7	48.4	227.0	52.2
90/10	45.2	91.0	166.5	43.3	224.1	48.5
80/20	45.8	95.5	162.5	43.0	218.7	45.6
70/30	46.2	99.0	157.8	39.6	213.9	41.3
30/70	49.1	109.2	154.3	14.8	211.5	19.3
20/80	50.6	113.4	151.0	11.0	210.2	14.2
10/90	54.5	118.0	149.0	4.9	207.5	8.3
PLA	62.0	–	–	–	–	–

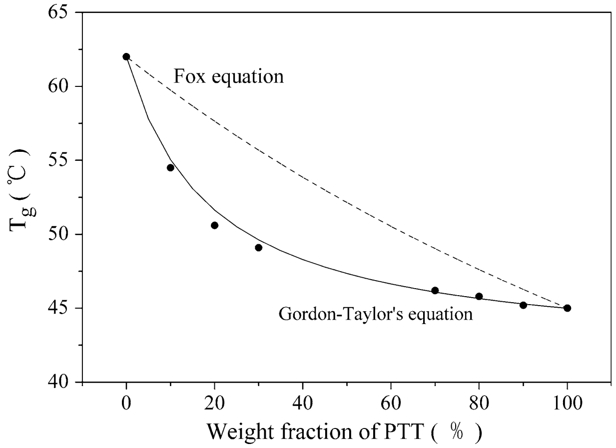

Fig. 2 Glass temperature (T_g) versus composition as Fox and Gordon–Taylor equations

$k = 0.91$, is in well agreement with the observed T_g values at all blend compositions.

The miscibility of the PTT/PLA blends in the amorphous phase could be evidenced by another thermal behavior, cold crystallization. A single and composition dependent cold-crystallization temperature (T_{cc}) can also exists for each sample, which is shown in Fig. 3 and listed in Table 1. The T_{cc} value of the blends remarkably increases as the PLA composition increases. Such a higher value of T_{cc} of the PTT/PLA blends means that PTT crystallization occurs later during the DSC heating scan and hence indicates a slower crystallization rate. That is to say, the PTT/PLA blends have a slower crystallization rate with increasing PLA content and the presence of PLA retards PTT crystallization. The chain mobility of PTT component is reduced owing to a slightly higher T_g when the PLA component is incorporated in the blends, which should account for the retarded PTT cold crystallization in the blends.

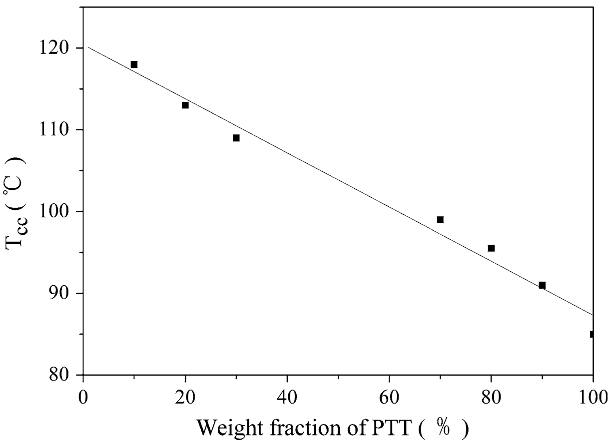

Fig. 3 Cold-crystallization peak (T_{cc}) in PTT/PLA blends

Melt crystallization and melting behavior of PTT/PLA blends

Figure 4a displays the DSC curves of PTT/PLA blends obtained from the first cooling scan. Apparently, an apparent exotherm is observed for PTT with a melt crystallization temperature (T_{mc}) at 186.7°, while no crystallization exotherm of the pure PLA appears under the same cooling rate of 10°/min. This result means that PTT with flexible molecular chains is more crystallizable than PLA, and the crystallization for PLA is almost inhibited at this cooling rate. For the PTT/PLA blends, each curve is shown with only one crystallization exothermic peak at lower temperature. Both T_{mc} and its exotherm ($\triangle H_{mc}$) values of the PTT/PLA blends are depressed with increasing PLA composition as shown in Table 1. This further supports the miscibility between PTT and PLA molecules in the melt. Furthermore, the crystallization exotherm becomes narrower and shifts to a lower temperature with increasing PLA content, indicating more retarded PTT crystallization.

The sequent melting thermograms for PTT, PLA, and the blends are shown in Fig. 4b. In fact, when the cooling rate is 10°/min, both the pure PTT and PTT/PLA blends cannot accomplish the crystallization during the cooling procedure and the recrystallization occurs again on the second heating. Therefore, on the thermogram recorded for pure PTT, there is exothermal peak followed by endothermal peak with a shoulder. Similar features can be found on the thermograms records for the PTT/PLA blends as illustrated in Fig. 4b. However, it is noticed that for pure PLA, no melting endothermic peak appears at the second heating as shown in Fig. 4b because of no melt crystallization at the first cooling scan. Furthermore, it can be seen that the melting temperatures of the blends in Fig. 4b show the same trend with the melt crystallization temperatures in Fig. 4a, i.e., the melting endotherms shift to a lower value and become narrower. Low crystallization temperature leads to relatively thin crystals and low melting point. The melting temperature and the exotherm ($\triangle H_m$) slightly decrease with increasing PLA composition, implying that the introduction of PLA component disturbs the crystallization of PTT, leads to

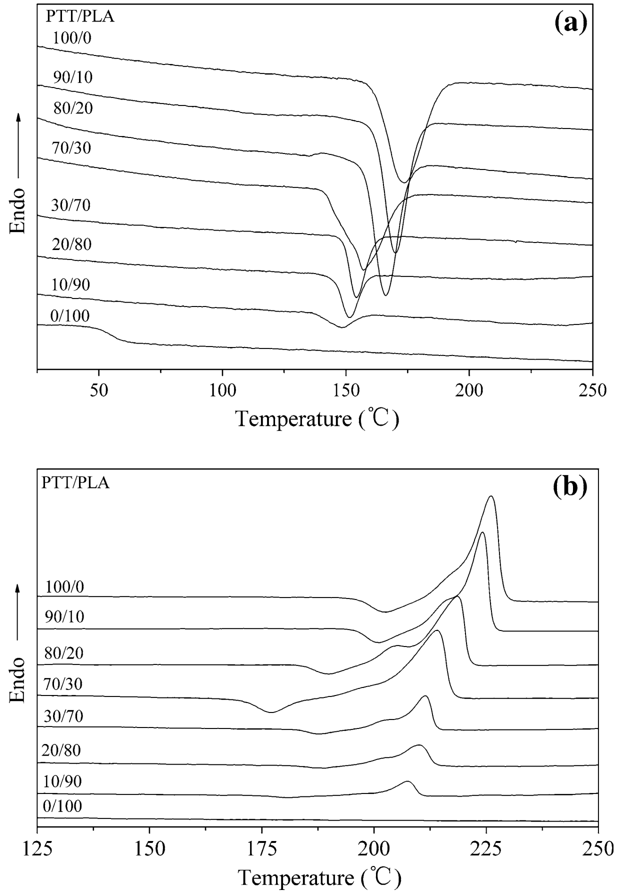

Fig. 4 DSC curves of PTT/PLA blends **a** the first cooling from the molten state at 10 °C/min, **b** the second heating at 10 °C/min

relatively thin and imperfect crystals, therefore, results in relatively low melting point.

Wide-angle X-ray diffraction analysis of PTT/PLA blends

Figure 5 shows the WAXD patterns of PTT, PLA, and PTT/PLA blends after annealing at 120 °C for 6 h. The characteristic X-ray peaks for PTT homopolymer are observed at the scattering angles 2θ of 15.3°, 16.8°, 19.4°, 23.6°, and 24.6°, which correspond to the diffraction planes of (010), $(0\bar{1}2)$, (012), (102) and $(1\bar{1}3)$, respectively [23]. The major characteristic X-ray peaks of PLA show two strong diffraction peaks at 2θ of 16.58° and 18.89°, assigned to the (200)and (203) reflections, respectively. The X-ray diffraction patterns of pure PLA are similar to those reported by Li et al. [24]. It is deem that PLA is able to crystallize after annealing at 120° for 6 h. However, at cooling rate of 10°/min, pure PLA is none

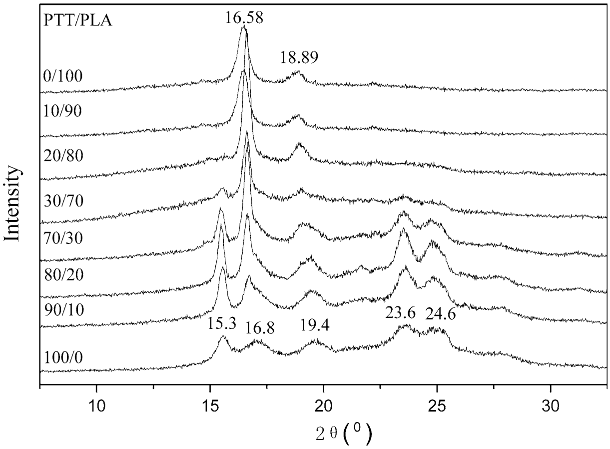

Fig. 5 WAXD patterns for PTT/PLA blends after annealing at 120 °C for 6 h

crystallizable just as illustrated previously, hence, no crystallization exothermic peak and melting endothermic peak can be observed in DSC curves of Fig. 4. That is to say, a 10 °C/min cooling process can't generate enough PLA crystals because PLA is a slower crystallizing polymer [25].

Apparently, apart from the major characteristic peaks of the pure PTT and PLA, no new peaks are observed in the diffraction patterns of the PTT/PLA blends. It could be concluded that the PTT and PLA components do not co-crystallize in the copolymers. Furthermore, the crystalline diffraction peaks of the PTT-rich blends are characterized by X-ray spectra which well match those of the PTT crystal structure, indicating that the crystalline phase present is that of PTT. On the contrary, the X-ray spectra of the PLA-rich blends are very similar to that of PLA, the position of the reflections being essentially the same and no evidence of a variation in the unit cell volume being found. These results prove that the crystal structure which develops in the PLA-rich blends corresponds to the characteristic lattice of the PLA. That is to say, the crystal structure which develops in the PTT/PLA blends is in consistent with the characteristic lattice of their enriched pure component.

Hydrolytic degradation of PTT/PLA blends

The hydrolytic degradation of PTT/PLA blends with the time is shown in Fig. 6. With prolonging the time from 7 days to 28 days, the weight loss of the PTT/PLA blends and pure PLA increases. To pure PLA, the value increases from 15.5% of 7 days to 27.5% for 28 days. However, to pure PTT, the weight does not change noticeably with extending the time. The weight loss of the PTT/PLA blends is between those of pure PTT and pure PLA. The higher the PLA content in the blends, the higher the weight loss at the same hydrolytic time (with the weight loss 17.0% of 30/70 blend, 20.3% of 20/80 blend, and 24.6% of 10/90 PTT/PLA blend after 28 days as shown in Fig. 6). Therefore, the incorporation of PLA segments into

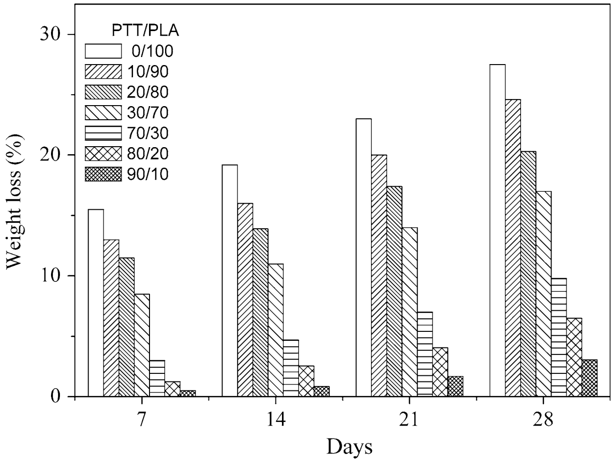

Fig. 6 Hydrolytic degradation study of PTT/PLA blends

PTT component is available to improve the hydrolytic degradation of PTT/PLA blends.

Mechanical properties of PTT/PLA blends

In Fig. 7, the tensile strength and elongation at break for pure PTT are 50.5 MPa and 24.6%, which is lower than the tensile strength of 55.8 and 58.3 MPa reported by Supaphol et al. [26] and Huang [18], respectively. Pure PLA film is found to be much more brittle with the values of 29.2 MPa and 10.0%, which agrees with the elongation at break reported by Peesan et al. [27]. Compared with the two pure components, the tensile strength and elongation at break of the PTT/PLA blends are intermediate. With the increase of PLA content, the tensile strength and the percentage of elongation at break of the PTT/PLA blend decrease. Physically, the PTT/PLA blend films have an inferior flexibility to pure PTT as PLA content increases.

Conclusions

A series of PTT/PLA blends were prepared by the melt blending. The blends exhibit a single, composition-dependent T_g at all compositions indicating that both PTT and PLA components are miscible in the amorphous state. The observed glass-transition temperature increases monotonically with increasing PLA content and is fitted well with the Gordon–Taylor equation, with the fitting parameters k being 0.91. The cold-crystallization peak temperature increases, while the melt-crystallization peak decreases with increasing the PLA content, suggesting that the presence of PLA in the blends retards the crystallization of PTT. Both the pure PTT and PTT/PLA blends cannot accomplish the crystallization during the cooling procedure and the recrystallization occurs again on the second heating. Therefore, on the thermogram

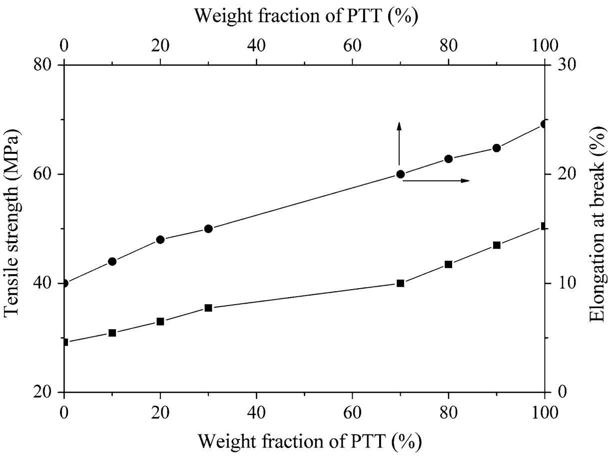

Fig. 7 Tensile strength and elongation at break for PTT, PLA, and the blends

recorded, there is exothermal peak followed by endothermal peak with a shoulder. The melting temperature and the melting enthalpy slightly decrease with increasing PLA composition. However, to pure PLA, no crystallization takes place during cooling from the melt, therefore, no melting endothermic peak is found on the second heating curve. The WAXD analysis indicated PTT and PLA components do not co-crystallize. The crystal structures which develop in the blends correspond to the characteristic lattice of their enriched component. With increasing PLA content, the hydrolytic degradation of the PTT/PLA blend films enhances, while both the tensile strength and the percentage of elongation at break of the blends descend.

Acknowledgments The financial support from the Scientific Research Foundation of Hubei Provincial Education Department (No: B200717003) and the Research Foundation of Wuhan University of Science and Engineering in China (No. 20073202) is greatly appreciated.

References

1. Bhuvanesh G, Nilesh R, Hilbornb J (2007) Poly(lactic acid) fiber: an overview. Prog Polym Sci 32:455–482
2. Ikada Y, Tsuji H (2000) Biodegradable polyesters for medical and ecological applications. Macromol Rapid Commun 21:117–132
3. Anderson JM, Shive MS (1997) Biodegradation and biocompatibility of PLA and PLGA microspheres. Adv Drug Deliv Rev 28:5–24
4. Jamshidi K, Hyon SH, Ikada Y (1988) Thermal characterizaton of polylactides. Polymer 29:2229–2234
5. Acar I, Özgümüş S, Kaşgöz A (2006) Nonisothermal crystallization kinetics and morphology of poly(ethylene terephthalate) modified with poly(lactic acid). Polym Plast Technol 45:351–359
6. Anderson KS, Hillmyer MA (2004) The influence of block copolymer microstructure on the toughness of compatibilized polylactide/polyethylene blends. Polymer 45:8809–8823
7. Narendra R, Digvijay N, Yang YQ (2008) Polylactic acid/polypropylene polyblend fibers for better resistance to degradation. Polym Degrad Stab 93:233–241
8. Biresaw G, Carriere C (2002) Interfacial tension of polylactic acid/polystyrene blends. J Polym Sci B Polym Phys 40:2248–2258

9. Hu Y, Rogunov M, Topolkaraev V et al (2003) Aging of poly(lactide)/poly(ethylene glycol) blends. Part 1. Poly(lactide) with low stereoregularity. Polymer 44:5701–5710
10. Xu H, Wang LH, Teng CQ et al (2008) Biodegradable composites: ramie fibre reinforced PLLA–PCL composite prepared by in situ polymerization process. Polym Bull 61:663–670
11. Zhang GB, Zhang JM, Wang SG et al (2003) Miscibility and phase structure of binary blends of polylactide and poly(methyl methacrylate). J Polym Sci Part B Polym Phys 41:23–30
12. Su ZZ, Guo WH, Liu YJ et al. (2009) Non-isothermal crystallization kinetics of poly(lactic acid)/modified carbon black composite. Polym Bull 62:629–642
13. Fathilah A, Chang YW, Kang SC (2009) Thermal, mechanical and rheological properties of poly(lactic acid)/epoxidized soybean oil blends. Polym Bull 62:91–98
14. Guerric EG, Eguiazábal JI, Nazabal (2007) Influence of compatibilization on the mechanical behavior of poly(trimethylene terephthalate)/poly(ethylene-octene) blends. J Eur Polym 43:1027–1037
15. Run MT, Wang YJ, Yao CG et al (2006) Non-isothermal crystallization kinetics of poly(trimethylene terephthalate)/poly(ethylene 2,6-naphthalate) blends. Thermochim Acta 447:13–21
16. Krutphun P, Supaphol P (2005) Thermal and crystallization characteristics of poly(trimethylene terephthalate)/poly(ethylene naphthalate) blends. Eur Polym J 41:1561–1568
17. Jafari SH, Yavari A, Asadinezhad A et al (2005) Correlation of morphology and rheological response of interfacially modified PTT/m–LLDPE blends with varying extent of modification. Polymer 46:5082–5093
18. Huang JM (2003) Polymer blends of poly(trimethylene terephthalate) and polystyrene compatibilized by styrene–glycidyl methacrylate copolymers. J Appl Polym Sci 88:2247–2252
19. Xue ML, Sheng J, Chuah HH et al (2004) Miscibility, morphology, and crystallization behavior of PTT/PC blends. J Macromol Sci Part B Polym Phys 43:1045–1061
20. Liang H, Xie F, Guo FQ et al (2008) Non-isothermal crystallization behavior of poly(ethylene terephthalate)/poly(trimethylene terephthalate) blends. Polym Bull 60:115–127
21. Liang H, Xie F, Chen B et al (2008) Miscibility and melting behavior of poly(ethylene terephthalate)/poly(trimethylene terephthalate) blends. J Appl Polym Sci 107:431–437
22. Brostow W, Chiu R, Kalogeras MI (2008) Prediction of glass transition temperatures: binary blends and copolymers. Mater Lett 62:3152–3155
23. Sirmoaon P, Dangseeyun N, Supaphol P (2004) Multiple melting behavior in isothermally crystallized poly(trimethylene terephthalate). Eur Polym J 40:599–608
24. Li HD, Nie W, Deng C (2009) Crystalline morphology of poly(L-lactic acid) thin films. Eur Polym J 45:123–130
25. Acar I, Durmuş A, Özgümüş S (2007) Nonisothermal crystallization kinetics and morphology of poly(ethylene terephthalate) modified with poly(lactic acid). J Appl Polym Sci 106:4180–4191
26. Supaphol P, Dangseeyun N, Thanomkiat P (2004) Thermal, crystallization, mechanical, and rheological characteristics of poly(trimethylene terephthalate)/poly(ethylene terephthalate) blends. J Polym Sci Polym Phys 42:676–686
27. Peesan M, Supaphol P, Rujiravanit R (2005) Preparation and characterization of hexanoyl chitosan/polylactide blend films. Carbohydr Polym 60:343–350